the plant journal

SEB Society for Experimental Biology

The Plant Journal (2018) **96,** 487–502 doi: 10.1111/tpj.14043

Principles and characteristics of the Arabidopsis WRKY regulatory network during early MAMP-triggered immunity

Rainer P. Birkenbihl[1,*], Barbara Kracher[1], Annegret Ross[1,†], Katharina Kramer[2], Iris Finkemeier[2,‡] and Imre E. Somssich[1,*]

[1]*Department of Plant Microbe Interactions, Max Planck Institute for Plant Breeding Research, Carl-von-Linné Weg 10, 50829, Cologne, Germany, and*

[2]*Plant Proteomics, Max Planck Institute for Plant Breeding Research, Carl-von-Linné Weg10, 50829, Cologne, Germany*

Received 1 June 2018; revised 6 July 2018; accepted 10 July 2018; published online 25 July 2018.

*For correspondence (e-mails birkenbi@mpipz.mpg.de; somssich@mpipz.mpg.de).

†Current address: Max Planck Institute for Biology of Ageing, Joseph-Stelzmann-Str. 9b, 50931, Cologne, Germany.

‡Current address: Institute of Plant Biology and Biotechnology, University of Muenster, Schlossplatz 7, 48149, Muenster, Germany.

SUMMARY

During microbe-associated molecular pattern-triggered immunity more than 5000 Arabidopsis genes are significantly altered in their expression, and the question arises, how such an enormous reprogramming of the transcriptome can be regulated in a safe and robust manner? For the WRKY transcription factors (TFs), which are important regulators of numerous defense responses, it appears that they act in a complex regulatory sub-network rather than in a linear fashion, which would be much more vulnerable to gene function loss either by pathogen-derived effectors or by mutations. In this study we employed RNA-seq, mass spectrometry and chromatin immunoprecipitation-seq to find evidence for and uncover principles and characteristics of this network. Upon flg22-treatment, one can distinguish between two sets of WRKY genes: constitutively expressed and induced WRKY genes. Prior to elicitation the induced WRKY genes appear to be maintained in a repressed state mainly by the constitutively expressed WRKY factors, which themselves appear to be regulated by non-WRKY TFs. Upon elicitation, induced WRKYs rapidly bind to induced WRKY gene promoters and by auto- and cross-regulation build up the regulatory network. Maintenance of this flg22-induced network appears highly robust as removal of three key WRKY factors can be physically and functionally compensated for by other WRKY family members.

Keywords: flagellin22, transcription factor regulatory network, W-box motif, WRKY target genes, *Arabidopsis thaliana*.

INTRODUCTION

During co-evolution with diverse pathogens plants have developed a highly complex and sophisticated innate immune system. A large array of plasma membrane-localized receptors recognize diverse microbe-associated molecular patterns (MAMPs) and thereby trigger appropriate signaling within a deeply interconnected network that ultimately enables proper transcriptional defense outputs (Tsuda and Somssich, 2015; Li *et al.*, 2016a; Yu *et al.*, 2017). Transcription factors (TFs) are among the most largely expanded gene families in plants, and this is also manifested in the increasing number of genes encoding defense-associated TFs including WRKY factors (Lehti-Shiu *et al.*, 2017). The number of WRKY genes increased drastically from only one or two genes in green algae, 19–38 in liverworts and mosses, and expanded up to more than 160 in flowering plants (Mohanta *et al.*, 2016) This expansion is clearly correlated with the multiple levels at which WRKY TFs operate within the complex MAMP-triggered and effector-triggered defense signal transduction cascades (Rushton *et al.*, 2010; Banerjee and Roychoudhury, 2015). Effector-triggered immunity (ETI) involves detection of specific virulence factors (effectors) mainly by dedicated intracellular host proteins thereby initiating a robust immune response (Cui *et al.*, 2015).

The growing numbers of WRKY factors enabled the plants to establish a very robust WRKY regulatory network due to high functional redundancy between the family members.

In *Arabidopsis thaliana* the WRKY TF gene family consists of 74 genes that can be sorted into subgroups based on the number and structure of the encoded conserved DNA-binding WRKY domains, which include the peptide sequence WRKYGQK and a Zn-finger motif (Eulgem *et al.*, 2000; Duan *et al.*, 2007). WRKY TFs exert their regulatory

functions by binding mainly to a DNA sequence (TTGACT/C) termed the W-box. Although it is known that also the W-box surrounding nucleotides have some influence on binding efficiency (Ciolkowski *et al.*, 2008) and in a few instances alternative WRKY binding sequence motifs have been uncovered (Sun *et al.*, 2003; van Verk *et al.*, 2008; Zhou *et al.*, 2018), it remains an enigma how distinct members of this large and heterogeneous TF family modulate proper context-dependent transcriptional outputs mainly by binding to the W-box.

From numerous expression studies in Arabidopsis, it became evident that nearly all WRKY family members (72 out of 74) are expressed, and the majority can be transcriptionally activated upon pathogen challenge or under abiotic stress conditions. Based on sequence inspection many of the Arabidopsis WRKY genes harbor several W-boxes within their regulatory regions, suggesting that WRKY factors may be involved in modulating WRKY gene expression. Indeed, already Eulgem *et al.* (1999) provided functional support for this assumption, revealing that activation of parsley *PcWRKY1*, which is involved in early host defense responses triggered by a cell-wall-derived oomycete elicitor, is mediated by a specific arrangement of W-boxes within its promoter region. Subsequent *in vivo* chromatin immunoprecipitation (ChIP) assays uncovered two intriguing details, namely that: (i) upon transcriptional activation, WRKY factors can bind to their own native promoters indicating feedback regulation; and (ii) that functionally important W-box elements required for gene activation are bound by distinct WRKY TFs in the induced state while they are pre-occupied by other WRKY TFs in the uninduced state (Turck *et al.*, 2004). The exchange of WRKY factors upon elicitation is in agreement with our previous work demonstrating that some defense gene promoters were already bound by WRKY proteins different from WRKY33 prior to inoculation with *Botrytis cinerea* spores, while WRKY33 bound to these sites after infection (Birkenbihl *et al.*, 2012). These and other findings led to the hypothesis that WRKY TFs not only act in combination with other TFs to modulate overall transcriptional immune outputs, but also form a regulatory sub-network in which functionally interconnected members of the family act via positive and negative feedback mechanisms to tightly control various defense pathways (Ülker and Somssich, 2004; Eulgem and Somssich, 2007; Pandey and Somssich, 2009).

Over the past few years, extensive studies in Arabidopsis and rice have provided further support to this hypothesis (Berri *et al.*, 2009; Choura *et al.*, 2015). In rice, the transcriptional repressor OsWRKY13 involved in cross-talk between abiotic and biotic stress signaling pathways was shown to target *in vivo* the promoters of *OsWRKY45-1*, *OsWRKY45-2* and *OsWRKY42*, as well as its own native promoter (Tao *et al.*, 2009; Xiao *et al.*, 2013; Cheng *et al.*, 2015). OsWRKY6 influences resistance to *Xanthomonas oryzae* pv. *oryzae* by directly targeting and positively regulating *OsWRKY6* gene expression (Choi *et al.*, 2015), whereas OsWRKY53, an important regulator of brassinosteroid signaling, directly targets and negatively regulates *OsWRKY53* expression (Tian *et al.*, 2017). In pepper, CaWRKY22 is a positive regulator of resistance toward *Ralstonia solanacearum* (Hussain *et al.*, 2018). CaWRKY22 binds to the promoter of *CaWRKY40* and also upregulated the expression of *CaWRKY6* and *CaWRKY27*, while downregulating *CaWRKY58*. Similarly, in Arabidopsis, AtWRKY33 targets its own gene promoter in a positive feedback loop required for resistance to *B. cinerea* (Mao *et al.*, 2011). AtWRKY10/MINI3 binds to its own gene promoter and thereby recruits a co-factor, SHB1, that is important for seed cavity enlargement (Kang *et al.*, 2013). The At*WRKY49* gene promoter was identified as an *in vivo* target of the immune regulator AtWRKY22 (Hsu *et al.*, 2013). Moreover, two WRKY factors, AtWRKY12 and AtWRKY13, that oppositely regulate flowering under short-day conditions, directly target each other's gene promoter (Li *et al.*, 2016b). Finally, during abscisic acid (ABA) signaling, AtWRKY40 was shown *in vivo* not only to bind to its own gene promoter, but also to the promoters of its closest related family members At*WRKY18* and At*WRKY60* (Yan *et al.*, 2013).

Arabidopsis WRKY18, WRKY33 and WRKY40 were shown to play distinct roles in plant immunity. WRKY33 function is critical for defense toward *B. cinerea* (Zheng *et al.*, 2006). WRKY33 also interacts with the MAP kinase substrate MKS1 thereby impacting host defense responses upon bacterial infection (Andreasson *et al.*, 2005; Qiu *et al.*, 2008). WRKY18 and WRKY40 were shown to act redundantly to negatively regulate resistance toward the powdery mildew fungus *Golovinomyces orontii*, but to positively affect AvrRPS4 ETI (Schön *et al.*, 2013). *wrky18 wrky40* double-mutant plants showed enhanced susceptibility toward the insect herbivore *Spodoptera litoralis*, but reduced colonization of their roots by *Trichoderma asperelloides* (Brotman *et al.*, 2013; Schweizer *et al.*, 2013). Moreover, *wrky18 wrky40* plants were more resistant to the virulent pathogen *Pseudomonas syringae* DC3000 (Xu *et al.*, 2006; Lozano-Durán *et al.*, 2013).

The extent of WRKY factors directly targeting diverse members of the WRKY gene family upon stimulation was recently demonstrated by two genome-wide studies employing ChIP-seq. During the early interaction of Arabidopsis with the fungus *B. cinerea* AtWRKY33 was shown to target its own gene promoter and 18 additional WRKY gene loci (Liu *et al.*, 2015). In the case of MAMP-triggered immunity (MTI), treatment of Arabidopsis seedlings with flg22, a peptide derived from the bacterial flagellum (Felix *et al.*, 1999), revealed binding of AtWRKY18, AtWRKY33 and AtWRKY40 to 22, 20 and 27 WRKY gene loci, respectively, within the first 2 h post-elicitation (Birkenbihl *et al.*,

2017). Although promoter binding by these TFs at the investigated time point did not always alter target gene expression, in many cases binding was associated with either activation or repression suggesting extensive positive and negative auto- and cross-regulation.

In this study a genome-wide systematical approach was undertaken to investigate the WRKY regulatory network of early MTI. By employing RNA-seq, mass spectrometry (MS) and ChIP-seq, we analyzed the consequences of flg22 elicitation on WRKY gene expression, WRKY protein abundances and WRKY factor binding to WRKY gene promoters. This analysis revealed that constitutively expressed WRKYs seem to be repressors of flg22-induced WRKY genes, and to be replaced by induced WRKYs upon elicitation, which then build up the network by WRKY factor cross- and auto-regulation. We also show that the network was capable to compensate for the removal of the three highly interconnected WRKY factors WRKY18, WRKY40 and WRKY33 (Choura *et al.*, 2015) by replacing them with other WRKY TFs, thereby maintaining functionally flg22-induced resistance toward the virulent bacterium *Pst* DC3000.

RESULTS

The WRKY regulatory network of early MTI comprises both constitutively expressed and induced WRKY factors

To assess the complexity and dynamics of the WRKY TF regulatory network of early MTI we first analyzed dynamics in the expression levels of WRKY genes and the abundances of WRKY proteins upon MAMP treatment. For WRKY transcript level analysis we used previously generated RNA-seq data (Birkenbihl *et al.*, 2017), which were based on RNA prepared from wild-type (WT) Col0 seedlings grown in liquid MS medium for 12 days, before they were treated for 1 or 2 h with the well-characterized MAMP flg22.

Two hours after flg22-treatment, 44 of the 74 Arabidopsis WRKY genes were clearly expressed above a threshold of four counts per million sequencing reads (cpm), which corresponded to about 100 reads in a sequenced library. Based on their expression dynamics, the WRKY genes were separated into two groups. Twenty-seven of the WRKY genes were clearly induced upon flg22-treatment more than twofold, while 17 were more-or-less constitutively expressed upon treatment with similar transcript levels upon treatment as in non-treated plants. Only two WRKY genes, *WRKY49* and *WRKY70*, were downregulated more than twofold upon flg22-treatment. The expression levels of the different WRKY genes varied strongly, with induced *WRKY33*, *11*, *6*, *15*, *40* and *29* reaching the highest levels at 1 or 2 h post-treatment (Figure 1a; Table S1).

In general, the RNA levels of the induced WRKY genes upon treatment reached significantly higher levels than the transcript levels detected for the constitutively expressed WRKY genes. For several WRKY genes the highest corresponding RNA levels were already found 1 h after flg22-treatment, suggesting that their functions may be related to early regulatory processes initiated prior to 2 h. Interestingly, among the constitutively expressed WRKY genes members of group I containing two WRKY domains were clearly overrepresented (Fisher test; $P = 0.012$; underlined in Figure 1; Eulgem *et al.*, 2000).

Dynamics of WRKY protein levels during early microbe-associated molecular pattern-triggered immunity

Because the regulatory capacity of a TF often correlates with its abundance, and RNA levels of certain genes may not necessarily reflect the abundance of their respective proteins, we also monitored the dynamics of WRKY factor protein levels upon flg22 elicitation. For this, nuclear extracts of WT seedlings, non-treated or treated with flg22 for 2–h, were analyzed by MS. To enrich for WRKY proteins, an affinity enrichment-mass spectrometry analysis (AE-MS; Keilhauer *et al.*, 2015) was performed employing an antibody directed against the highly conserved WRKY domain (designated anti-all-WRKY) potentially binding to most WRKY proteins (Turck *et al.*, 2004).

Following the AE-MS analysis using the anti-all-WRKY antibody, 26 different WRKY proteins were detected and quantified in the lysates of non-treated seedlings, while only four of them were detected at background levels and in single replicates in pull-downs using the pre-immune serum. The protein quantification of the enriched WRKY proteins is based on a label-free quantification algorithm (MaxLFQ) that uses more than 700 detected proteins in five independent biological replicates, which bind mainly unspecifically to the antibody agarose for normalization. The validity of this quantification approach is furthermore indicated by the high Pearson correlation (> 0.8) of LFQ intensities between samples from the 0 and 2 h experiments. The same WRKY proteins and additionally WRKY30 were identified in the immunoprecipitates (IPs) of lysates from flg22-treated seedlings (Figure 1b; Table S2). For 14 of them, WRKY6, 8, 11, 18, 22, 25, 28, 29, 30, 33, 40, 48, 53 and 75 (all belonging to the group of induced WRKY genes on the RNA level), the protein levels were statistically significantly elevated after flg22-treatment by more than twofold (WRKY45 only 1.5-fold) compared with their levels in non-treated seedlings. From this group only WRKY7, WRKY45 and WRKY47 had slightly reduced or similar levels upon flg22-treatment as in non-treated seedlings, respectively. The protein levels of 10 WRKY proteins, belonging to the constitutively expressed WRKY genes, WRKY1, 3, 4, 19, 20, 26, 32, 57, 60 and 69, did not change in abundance upon flg22-treatment. Thus, the analysis of WRKY protein levels showed a similar induction pattern as found for their RNA transcripts thereby confirming the

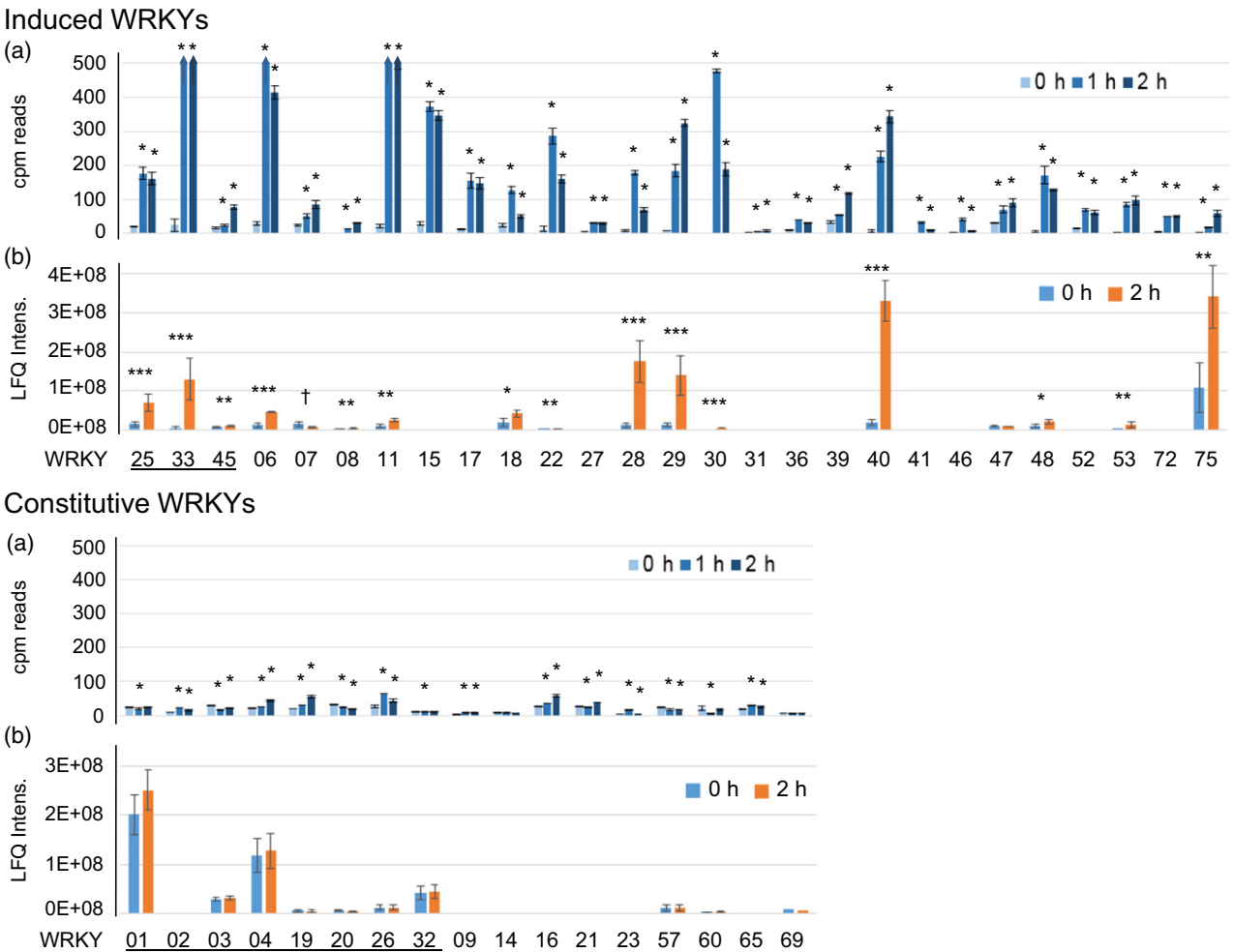

Figure 1. Flg22-induced and constitutively expressed WRKY factors. (a) WRKY transcript levels. Arabidopsis seedlings were mock-treated (0 h), or treated for 1 or 2 h with flg22, and total RNA isolated for RNA-seq. Shown are counts per million sequencing reads (cpm) for the three time points for each WRKY gene indicated underneath. WRKY genes belonging to group I are underlined. Error bars represent the standard deviation of three replicates. Significant changes in expression upon treatment were calculated by moderated *t*-test with samples below a 0.05 *P*-value cutoff marked with an asterisk. All numbers, including overshooting values, are listed in Table S1. (b) WRKY protein levels. WRKY proteins in nuclear lysates from seedlings, non-treated or treated for 2 h with flg22, were enriched by IP using the anti-all-WRKY antibody and subsequently identified and quantified by mass spectrometry (MS). Displayed are average label-free quantification (LFQ) intensities with standard deviations from five independent biological replicates. *P*-values from Student's *t*-test statistics are indicated as follows: $^{\dagger}P < 0.1$, $*P < 0.05$, $**P < 0.01$, $***P < 0.001$ (related to Table S2). Data from individual replicates can be found in Data S1.

classification of the WRKY genes into the two sets, induced and constitutively expressed WRKY genes (Figure 1b).

Some WRKY genes with relative high transcript levels, such as *WRKY15* and *WRKY17* for the induced, and *WRKY16* for the constitutively expressed WRKY genes, were not detected on the protein level. Reasons for this could be that their protein amounts were just below the detection limit, or that they were not bound by the anti-all-WRKY antibody and thus not enriched for MS analysis.

Beside confirming the two sets of constitutively expressed and induced WRKY factors also on the protein level, this experiment gave us valuable information regarding the capability of the anti-all-WRKY antibody to recognize many different WRKY proteins, which was important with respect to the use of this antibody for subsequent ChIP-seq studies.

WRKY factor binding to WRKY gene promoters

One central hypothesis underlying the WRKY regulatory network is that it involves extensive cross-regulation among many WRKY gene family members, and auto-regulation of single WRKY genes by means of positive or negative feedback loops.

From recent ChIP-seq experiments we extracted data showing which WRKY gene promoters were targeted by the strongly flg22-induced and highly expressed genes *WRKY18*, *WRKY40* and *WRKY33* (Birkenbihl *et al.*, 2017). In that study complementation lines expressing HA-tagged versions of *WRKY18*, *WRKY40* and *WRKY33* from their

own promoters in the respective knockout mutant lines were used as no high-quality WRKY-specific antibodies appropriate for ChIP-seq experiments existed. Binding sites for each of the three WRKY factors were determined by comparing site-specific accumulation of ChIP-seq reads of the three WRKY-HA lines with equally treated WT samples not containing HA-tagged proteins.

All three WRKY proteins bound to a set of about 30 WRKY genes (Birkenbihl *et al.*, 2017). This represents about 40% of all WRKY genes within the genome demonstrating that WRKY factor binding to this gene family was highly overrepresented compared with all targets, which represented only about 5% of all Arabidopsis genes. While there was some weak binding of WRKY18 due to low transgene expression also in the non-elicited state, WRKY33 and WRKY40 binding were almost exclusively observed after flg22-treatment. Binding of all three WRKY proteins was observed predominantly at the promoters of the induced WRKY genes and in nearly all instances to W-box motifs (TTGACT/C), the DNA element known to be bound by WRKY factors. The only constitutively expressed WRKY gene bound by all three WRKY factors was *WRKY60.* In almost all cases simultaneous binding of WRKY18 and WRKY40 was observed, consistent with the earlier observation that they can bind to DNA as heterodimers (Xu *et al.*, 2006). Moreover, each of the three WRKY proteins bound to its native gene promoter indicating potential feedback auto-regulation (Figure 2a; Table S3).

It has been reported that W-boxes are overrepresented in upstream regions of WRKY genes compared with all genes, which was taken as an indication that WRKY factors regulate WRKY genes (Dong *et al.*, 2003; Llorca *et al.*, 2014). We analyzed the 1500-bp upstream region of all WRKY genes, and found for the induced WRKY genes compared with the constitutively expressed WRKY genes W-boxes clearly enriched 3.8 versus 2.2 W-boxes (Figure S1). In line with this we observed at some promoters of the inducible WRKY genes, for example *WRKY6*, *11*, *15*, *17*, *18*, *40*, *48* and *53*, multiple binding peaks of the WRKY factors (Figure S3). *WRKY27*, *WRKY31*, *WRKY36* and *WRKY52*, even though belonging to the group of induced WRKY genes, were not bound by any of the three WRKY factors at the investigated time point. From this experiment we concluded that the induced WRKY factors WRKY18, WRKY40 and WRKY33 upon elicitation bind to most of the promoters of the flg22 inducible WRKY genes to regulate their expression.

To monitor potential binding by additional WRKY proteins besides WRKY18, WRKY40 and WRKY33, we performed ChIP-seq experiments on WT seedlings employing the anti-all-WRKY antibody, which was capable of recognizing at least 27 different WRKY proteins in our MS experiments. As expected, we observed WRKY factor binding to nearly the same set of induced WRKY gene promoters upon flg22-treatment, and again only binding to *WRKY60* of the constitutively expressed WRKY gene set. Intriguingly, however, binding now was also detected without flg22-treatment at the same sites (Figure 2b; Table S3), indicating that the WRKY promoter binding sites of the induced WRKY genes were already pre-occupied by WRKY factors different from WRKY18, WRKY40 and WRKY33 prior to elicitation.

To firmly exclude WRKY18, WRKY40 and WRKY33 binding, we subsequently used the same experimental setup on *wrky18 wrky40 wrky33* triple-mutant seedlings employing the anti-all-WRKY antibody for ChIP-seq. The detected binding pattern was basically the same as with WT seedlings, indicating that in the elicited state WRKY18, WRKY40 and WRKY33 had been replaced by other WRKY factors binding to the same WRKY promoter sites (Figure 2c).

The results from all ChIP-seq experiments are illustrated in Figure 2(d) using the Integrated Genome Viewer (IGV; Thorvaldsdóttir *et al.*, 2013). This visualization shows the detected WRKY binding peaks at the promoter of the induced *WRKY30* gene and co-localization of W-boxes with the positions of these peaks. Figure 3(a) provides an additional example from the promoter of induced *WRKY15*. Besides WRKY factor binding to expressed WRKY genes we also observed binding to six WRKY genes that were not expressed under the conditions we used (Figure 2).

Induced WRKY genes appear to be mainly regulated by WRKY factors, whereas this is not the case for the constitutively expressed WRKY genes

DNAse hypersensitive sites (DHSs) indicate locations of open chromatin mainly in promoters of actively transcribed genes (Jiang, 2015). These sites are accessible and can be bound by transcriptional regulators like TFs. Recently, genome-wide maps of DHSs have become available (Zhang *et al.*, 2012; Sullivan *et al.*, 2014). We compared the WRKY binding peak locations from our ChIP-seq experiments with a map of DHSs from non-treated Arabidopsis young leaf tissue (Zhang *et al.*, 2012) by integrating the DHS map positions into the IGV browser. This comparison revealed an almost perfect overlap of DHSs and WRKY binding sites for most of the induced WRKY genes. In most cases even the binding site peaks and centers of the DHSs co-localized and culminated at W-boxes, indicating occupation of these DHSs by WRKY factors, possibly functioning as transcriptional regulators of the associated WRKY genes. As an example, Figure 3(a) shows the locus of the induced *WRKY15* gene. Here three DHSs within the 2.5-kb region upstream of the transcription start site (TSS) align with the main WRKY binding sites and culminate at W-boxes. Because the 0 h data from ChIP-seq and the DHSs data were both derived from non-treated material, this indicates that already prior to elicitation these key regulatory sites are mainly occupied by WRKY factors.

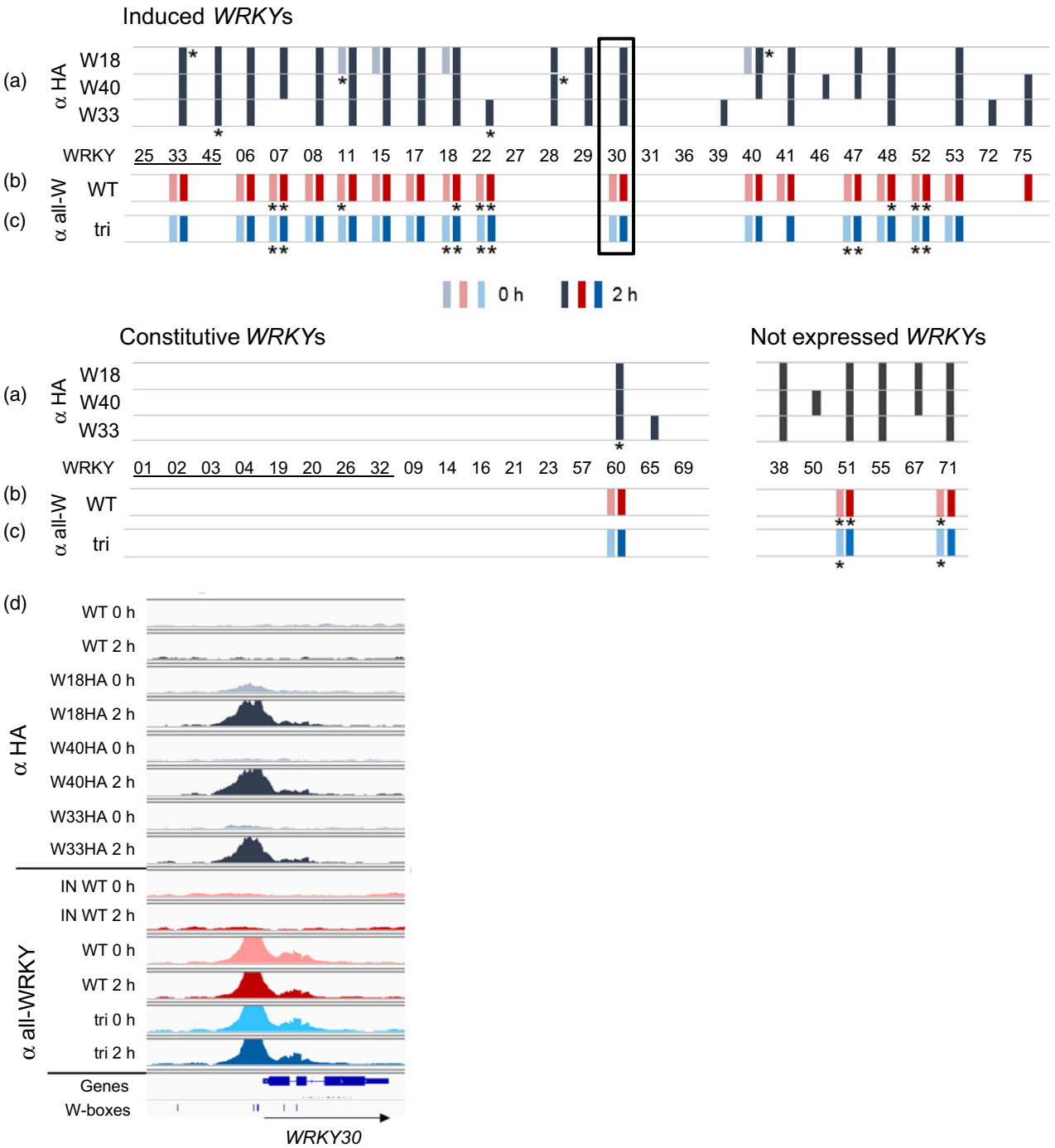

Figure 2. Flg22-elicited WRKY factor binding to induced and constitutively expressed WRKY genes. (a) WRKY18, WRKY40 or WRKY33 binding to WRKY genes. Complementation lines of the three WRKY genes expressing HA-tagged proteins were used for chromatin immunoprecipitation (ChIP)-seq on mock-treated (0 h) or seedlings treated for 2 h with flg22. Binding is indicated by bars above the targeted WRKY gene numbers. (b) Binding of potentially many WRKY factors to WRKY genes revealed by ChIP-seq using wild-type (WT) seedlings and the anti-all-WRKY antibody. (c) Binding of many WRKY factors except WRKY18, WRKY40 and WRKY33 to WRKY genes detected by ChIP-seq using a *wrky18 wrky40 wrky33* triple-mutant and the anti-all WRKY antibody. Bars marked with an asterisk symbolize binding judged by visual inspection from IGV browser images (Figure S3). (d) IGV-image of WRKY factor binding to the promoter of induced WRKY30. Shown are the binding peaks derived from the ChIP experiments indicated in (a)–(c) highlighted by a black frame (related to Table S3).

These WRKY factors must be different at least from WRKY40 and WRKY33, which showed binding only upon flg22-treatment. This assumption is further validated by the ChIP-seq data obtained with the *wrky18 wrky40 wrky33* triple-mutant (Figure 2c). Another DHS is localized at the 3′-end of *WRKY15*, which may represent an enhancer site

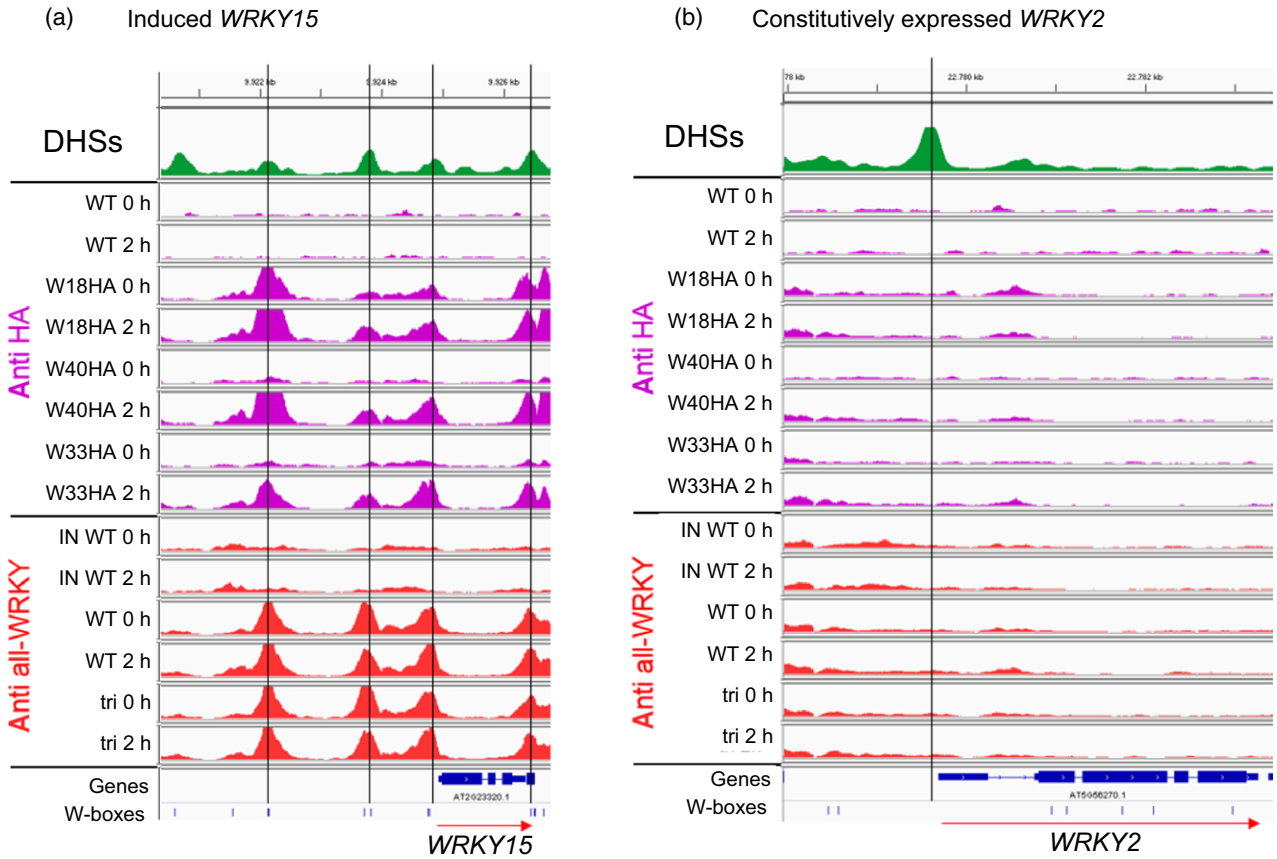

Figure 3. Co-localization of DNAse hypersensitive sites (DHSs) and WRKY factor binding sites at the promoters of the induced *WRKY15* (a) and the constitutively expressed *WRKY2* genes (b). Shown are IGV images of the binding peaks derived from the chromatin immunoprecipitation (ChIP) experiments indicated in Figure 2a–c underneath the DHSs peaks and above the gene loci. Positions of W-boxes are marked by vertical lines. DHS data were derived from Zhang *et al.* (2012).

also bound by WRKY factors. For 21 of the 27 induced WRKY genes we found DHSs within their promoter regions, which co-localize with WRKY binding peaks and W-boxes (Figure S3). This pronounced co-occurrence suggests that the induced WRKY genes are regulated mainly by WRKY factors.

The situation is clearly different at the gene loci of the constitutively expressed WRKY genes, as exemplified for the *WRKY2* gene locus shown in Figure 3(b). Here, one prominent DHS is located close to the TSS, indicative of a regulatory binding site. However, no WRKY factor binding is observed and this region lacks W-box motifs. Ten of the 17 loci of constitutively expressed WRKY genes show a similar constellation; three do have a DHS that co-localized with W-boxes but show no WRKY factor binding, and at three of the loci no DHS is observed. Only *WRKY60* has a DHS encompassing a W-box and also showed WRKY binding while its transcript levels remain unchanged 2 h post-flg22-treatment (Figure S3). Together these data suggest that the constitutively expressed WRKY genes, possibly excluding *WRKY60*, are almost exclusively modulated by non-WRKY-type transcriptional regulators.

In the non-elicited state flg22-induced WRKY genes are likely repressed by constitutively expressed WRKY factors

In an earlier study application of the protein biosynthesis inhibitor cycloheximide (CHX) to otherwise non-treated Arabidopsis seedlings revealed that more than 80% of all rapidly elicited flg22-responsive genes were transcriptionally induced (Navarro *et al.*, 2004). This suggests that these CHX-induced genes are under negative control by repressors with short half-lives that cannot be replenished when protein biosynthesis is blocked. In a different study employing Affymetrix ATH1 microarrays covering nearly 22 000 Arabidopsis genes, almost all of the flg22-induced WRKY genes identified here were among the CHX-induced genes, but only three of the constitutively expressed WRKY genes when applying a threshold of at least twofold upregulation (William *et al.*, 2004; Figure 4; Table S4). This implies that the flg22-induced WRKY genes are negatively regulated by protein factors. As our ChIP experiments

clearly detect WRKY binding in the non-elicited state predominantly at the promoters of the induced WRKY genes and these binding sites co-localized with major DHSs, this strongly suggests that repression of the flg22-induced WRKY genes in the non-elicited state is mainly established by the WRKY factors encoded by the constitutively expressed WRKY genes.

To further test this assumption we compared the transcript levels of induced WRKY genes in non-treated WT plants and plants carrying mutations in different constitutively expressed WRKY genes. Overall, there was a tendency that some induced WRKY genes are slightly higher expressed in some of the mutant plants (Table S5), suggesting negative regulation by the corresponding constitutively expressed WRKY gene. However, the fold changes in transcript levels were much lower than those observed upon CHX treatment or upon induction by flg22-treatment, while the standard deviations for the three replicates were rather large. Very likely functional genetic redundancy among the constitutively expressed WRKY genes is responsible for the weak effects observed. Thus, the generation of higher order mutants will be required to resolve this issue.

Robustness of the WRKY regulatory network

Upon elicitation, the expression of *WRKY18, WRKY40* and *WRKY33* is strongly induced and their encoded TFs rapidly bind to the promoters of most of the induced WRKY genes. Nevertheless, we showed that upon removal of all three factors from the WRKY regulatory network by using the *wrky18 wrky40 wrky33* triple-mutant, the corresponding binding sites in these promoters were now occupied by other WRKY factors (Figure 2c). To investigate whether the absence of these three WRKY genes from the WRKY network had a consequence on the induced transcript levels of all WRKY genes, we performed RNA-seq experiments

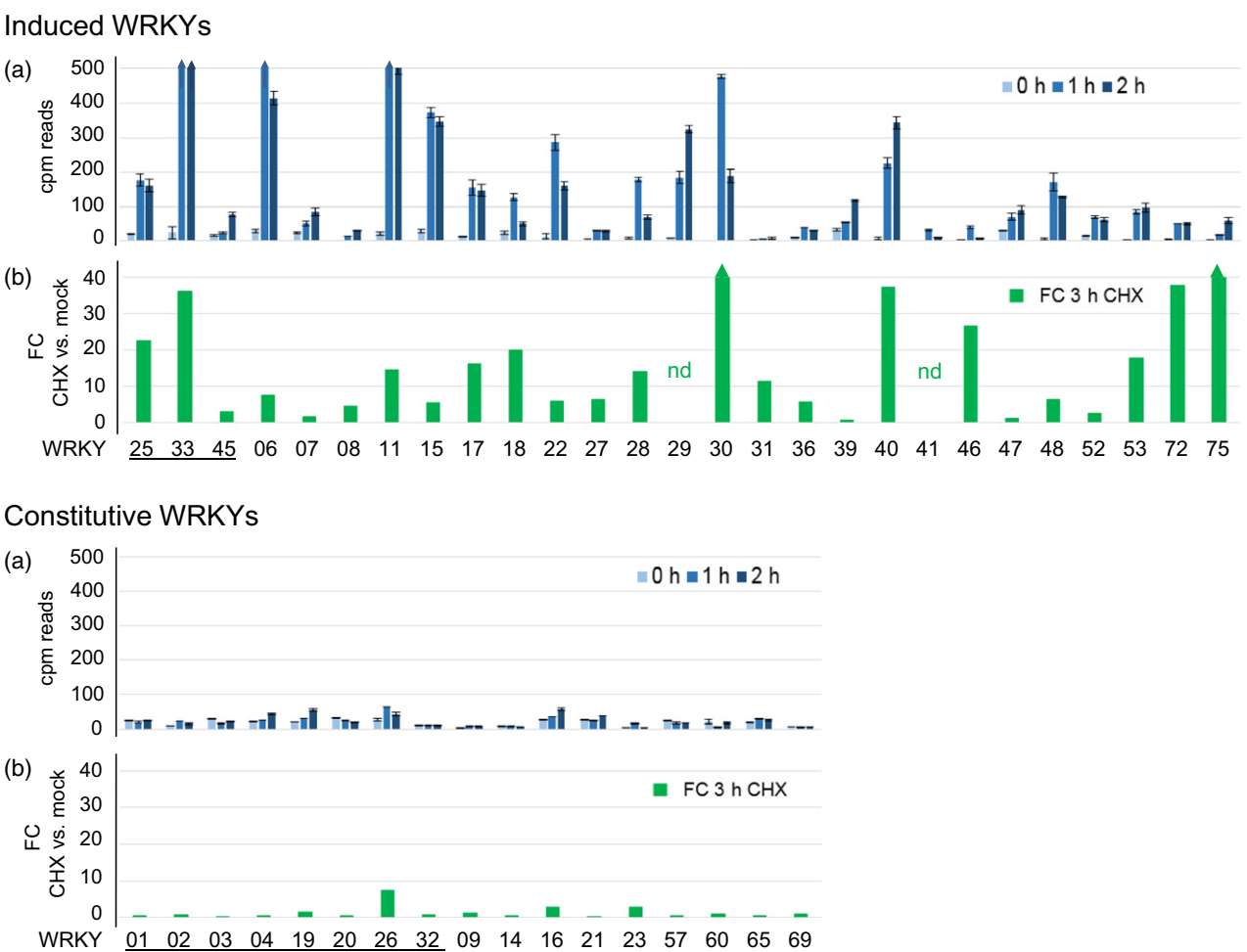

Figure 4. Comparison of transcriptional induction of WRKY genes by flg22 or cycloheximide (CHX). (a) Flg22-induced WRKY gene transcript levels derived by RNA-seq (same as in Figure 1a). (b) Fold changes of WRKY transcript levels from Arabidopsis seedlings treated with CHX for 3 h compared with mock-treated seedlings. The CHX data were extracted from previously published ATH-1 microarrays (William *et al.*, 2004). nd marks WRKY genes not present on the ATH-1 chip (related to Table S4).

comparing the expression levels of the WRKY genes between WT and the triple-mutant after 2 h flg22-treatment. Intriguingly, expression patterns of the WRKY genes remained the same in the triple-mutant and in WT seedlings with respect to flg22 inducibility and transcript levels (Figure 5; Table S6). Significant changes in transcript levels between the two genotypes were only observed for the three mutated WRKY genes. Even though we cannot completely exclude the possibility that the loss of *WRKY18*, *WRKY40* and WRKY33 was compensated for by some other TFs possibly binding to other sites, our experimental results suggest that they were replaced by other WRKY factors not only physically as shown by ChIP, but also functionally as seen by unaltered WRKY gene transcript levels highlighting the robustness of the WRKY network.

We also tested whether flg22-induced resistance toward virulent *P. syringae* (*Pst* DC3000) is altered in the *wrky18 wrky40 wrky33* triple-mutant compared with WT plants. *WRKY18*, *WRKY40* and *WRKY33* have been shown to be significantly upregulated upon *Pst* DC3000 inoculation (Microarray AT-00202 extracted from Genevestigator website) and to affect growth of this bacteria *in planta* (Zheng *et al.*, 2006; Lozano-Durán *et al.*, 2013). Four-week-old Arabidopsis Col-0 plants were first infiltrated with flg22 and 24 h later syringe infiltrated with the bacterium. The flg22-induced resistance phenotype was scored after 3 days and revealed no difference between the triple-mutant and WT, while *fls2* control plants were more susceptible (Figure 6). When we repeated this experiment, but this time with *Pst* spray inoculation, we got the same result (Figure S2). This is a further indication of the robustness of the WRKY regulatory network in MTI.

DISCUSSION

Our systematical analysis of the WRKY TF family potentially involved in early MTI identified two distinct sets of WRKY genes. One set, comprising 27 genes, showed enhanced expression within 2 h following flg22-treatment, and 15 of their encoded proteins showed elevated levels detected by MS upon elicitation. The second set, comprising 17 WRKY genes, showed more-or-less unaltered expression upon flg22-treatment, and 10 of their encoded proteins were also identified by MS and showed unaltered levels, justifying the separation of the expressed WRKY genes into the two groups also on the protein level. This classification of the two groups was also supported by the finding that all of the 19 flg22 upregulated WRKY genes detected in a previous report (Zipfel *et al.*, 2004) were also identified in our study as being upregulated. This categorization of the WRKY genes holds true also under pathogen infection conditions and under quite different experimental setups. In an extensive transcriptome analysis (Lewis *et al.*, 2015), 22 of the 27 induced WRKY genes were also induced 2 h after *Pst* DC3000 infiltration, while 15 of the 17 constitutively expressed WRKY genes in our study were also not induced (Table S8).

Detailed analysis of our previous ChIP-seq data (Birkenbihl *et al.*, 2017) for WRKY genes that were direct targets of three strongly and rapidly flg22-induced WRKY factors, WRKY18, WRKY40 and WRKY33, revealed that they predominantly target the promoters of the flg22-inducible WRKY genes including their own gene promoters upon elicitation. These findings are consistent with previous reports showing that WRKY gene promoters are enriched for W-boxes compared with all genomic gene promoters (Dong *et al.*, 2003; Llorca *et al.*, 2014), and with co-expression studies revealing that 70% of the Arabidopsis WRKY genes analyzed are co-regulated with other WRKY factors (Berri *et al.*, 2009; Choura *et al.*, 2015), suggesting extensive cross-regulation within this gene family. Moreover, several individual studies have clearly pointed to a functional linkage of many WRKY genes by auto- and cross-regulatory mechanisms (Eulgem and Somssich, 2007; Hu *et al.*, 2012; Yan *et al.*, 2013; Cheng *et al.*, 2015; Li *et al.*, 2016b), a hypothesis that has gained strong additional support by another recent genome-wide study in Arabidopsis (Liu *et al.*, 2015).

An intriguing but unresolved question is why do the three WRKY factors mainly target selected W-boxes within inducible WRKY gene promoters but not in the constitutive WRKY gene promoter set? We examined the W-box numbers in the 1500-bp upstream regions of all WRKY genes, and found that on average significantly more W-boxes are present within this region in the induced than in the constitutively expressed WRKY gene promoters (3.8 versus 2.2 motifs; $P = 0.00059994$; non-parametric bootstrap test with 10 000 iterations; Figure S1; Table S1). However, whether this difference in binding site numbers alone is sufficient to explain this discrepancy remains doubtful. Clustering of TF binding motifs for the same TFs, so-called homotypic clusters, within promoter-proximal regions and enhancers has been suggested to maintain transcriptional robustness and to preserve stress responsiveness against *cis*-regulatory mutations (Barah *et al.*, 2016). Interestingly, our ChIP-seq data show that there is not only a higher number of W-boxes in the promoters of induced WRKY genes, but also that in many cases several of these sites were bound by the WRKY factors (i.e. for *WRKY6*, *11*, *15*, *17*, *48*, *53*; Figure S3). Whether such binding additively or synergistically enhances expression or increases specificity remains to be determined. Note, however, that ChIP experiments cannot distinguish whether multiple WRKY factor molecules bind simultaneously to such a site on a single DNA molecule or whether different WRKY factors bind the same site on different DNA molecules originating from distinct cells.

Differences in the local topography of the genomic promoter regions between the two sets of WRKY genes and/or

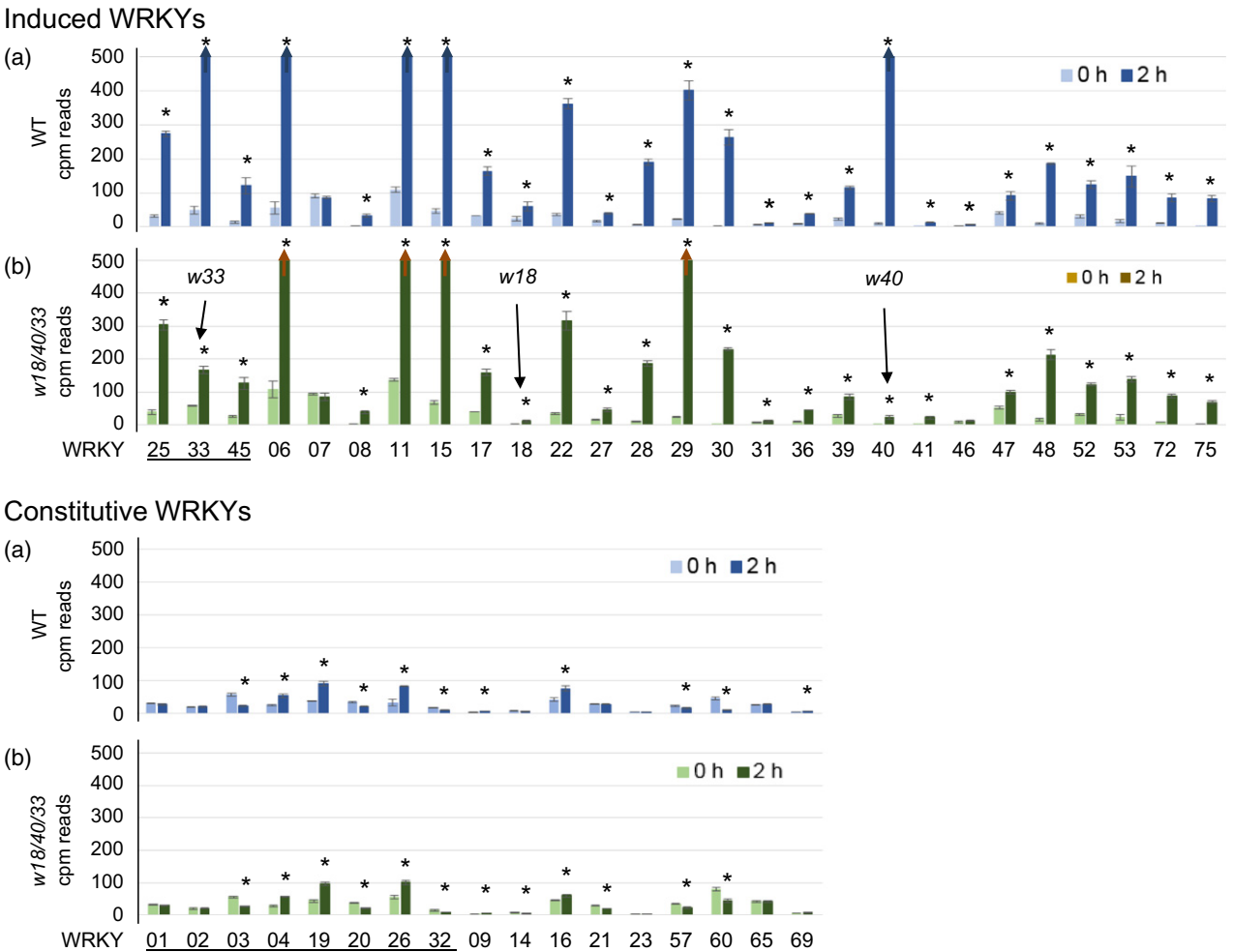

Figure 5. Flg22-induced WRKY gene expression in wild-type (WT) and in the *wrky18 wrky40 wrky33* triple-mutant. WT (a) and *wrky18 wrky40 wrky33* (b) total RNA from untreated (0 h) or 2 h flg22-treated seedlings were analyzed by RNA-seq. Indicated are counts per million sequencing reads (cpm) for the two time points and both genotypes. Arrows point to the mutated genes in the triple-mutant. Error bars represent the standard deviations of three replicates. Significant changes in expression upon treatment were calculated by moderated *t*-test with samples below a 0.05 *P*-value cutoff marked with an asterisk. All numbers are listed in Table S6.

a preference for distinct combinations of additional TF binding sites may also contribute to whether these genes are competent to respond to the MAMP flg22 or not. In this respect, it is interesting to note that the promoter of *WRKY71* contains numerous W-boxes and is bound by all three tested WRKY factors upon elicitation, yet it does not appear to be expressed (Figures 2 and S3). Thus, additional promoter properties seem to be required to enable flg22-induced gene expression. Furthermore, expression of several of the WRKY genes that fail to respond to flg22 elicitation have been demonstrated to be affected by other internal and external stimuli. For instance, *WRKY71* responds to abiotic stresses and promotes shoot branching and flowering (Guo and Qin, 2016; Yu *et al.*, 2016). Expression of *WRKY1*, *WRKY2* and WRKY57 is modulated by the phytohormone ABA (Jiang and Yu, 2009; Jiang *et al.*, 2012; Qiao *et al.*, 2016), and *WRKY57* is also induced by *B. cinerea* and *Pst* DC3000 infection (Jiang and Yu, 2016). *WRKY26* responds strongly to elevated temperature (Li *et al.*, 2011), while various abiotic treatments affect *WRKY3* and *WRKY4* expression (Lai *et al.*, 2008). Thus, these genes have the competence to respond to appropriate signals.

A key finding of our genome-wide study is that early MAMP-triggered upregulation at WRKY gene loci appears to involve rapid displacement of pre-bound WRKY repressors at functional W-box elements by activated WRKY family members. Such a mechanism has been proposed earlier based on a limited study in parsley (Turck *et al.*, 2004), but how general such a mechanism is remained unclear. It is important to note that WRKY factor binding in the non-elicited state was restricted to those same W-box motifs to which WRKY18, WRKY40 and WRKY33 subsequently bound upon flg22 stimulation. Our conclusion is

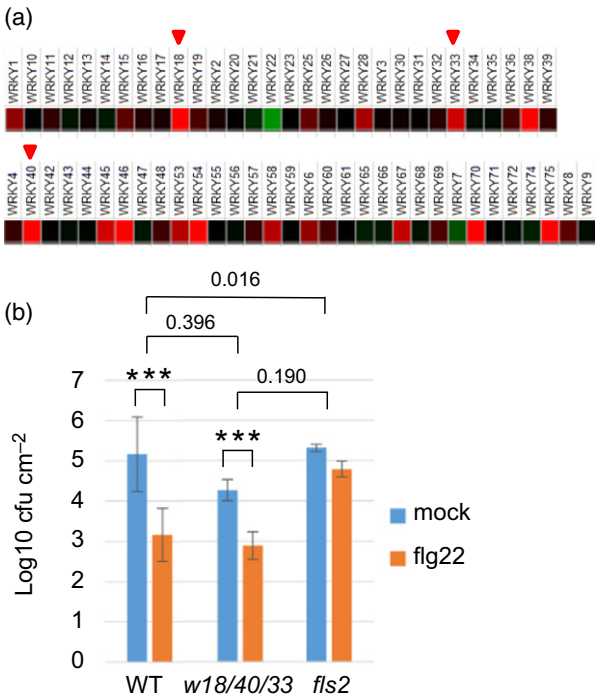

Figure 6. The *wrky18 wrky40 wrky33* mutant is still proficient in flg22-induced resistance. (a) WRKY18, WRKY40 and WRKY33 are significantly induced by *Pseudomonas syringae* pv. *tomato* (*Pst* DC3000). Shown are WRKY expression data following inoculation of Arabidopsis plants with *Pst* DC3000 derived from Microarray AT-00202 extracted from the Genevestigator website. (b) Flg22-induced resistance assay. Leaves of 4-week-old wild-type (WT), *wrky18 wrky40 wrky33* and *fls2* plants were syringe-infiltrated with flg22 or water (mock) 24 h before inoculation with *Pst* DC3000 via syringe infiltration. After 3 days bacterial titers were determined. Shown are the average numbers from six experiments. Error bars represent standard deviation. ***Indicates adj. *P*-values below 0.001 by ANOVA with *post hoc* tests for mock versus flg22. Numbers above square brackets represent *P*-values for the comparison of flg22 responses (i.e. difference flg22 versus mock) between genotypes computed by ANOVA and Tukey *post hoc* tests.

further supported by the fact that treatment of naive seedlings with the protein synthesis inhibitor CHX activated expression of almost all flg22-induced WRKY genes, but only three of the constitutively expressed ones (Figure 4; William *et al.*, 2004), indicating that the gross of the induced WRKY genes are under negative control by repressor proteins. Moreover, alignment of the WRKY binding sites in the promoters of the induced WRKY genes with the DHSs derived from naive young leaf tissue (Zhang *et al.*, 2012), which serves as a proxy for regions of open chromatin encompassing active enhancers (Zhu *et al.*, 2015), revealed for most promoters co-localization of DHSs with WRKY binding peaks and W-boxes (Figures 3 and S3). One must note, however, that CHX has been shown to exert additional modes of action independent of its protein synthesis inhibitor activity (Kim Do *et al.*, 2011; Brown *et al.*, 2012). Together these findings indicate that constitutively expressed WRKY factors participate in repressing the induced WRKY genes in the non-elicited state. An alternative model, although not mutually exclusive, could be that the WRKY factors form a platform at W-box promoter sites for additional regulatory co-factors. Such a platform would enable repressors to associate and restrict expression in the uninduced state while enabling new factors, including the induced WRKY factors, to displace certain repressive components from the complex upon induction by flg22. The constant presence of such WRKY complexes may also contribute to maintaining an open chromatin environment, which would be consistent with their co-localization to the observed DHSs.

In contrast, constitutively expressed WRKY gene promoters often reveal only one prominent DHS located close to the TSSs, which do not co-localize with W-boxes, indicating that regulatory proteins other than WRKY factors modulate and maintain their expression.

In our analysis, we observed WRKY factor binding only to a fixed set of W-boxes that account for less than 5% of the nearly 140 000 W-boxes present in the Arabidopsis genome. This became obvious when employing the anti-all-WRKY antibody in ChIP assays. Basically, the same binding patterns emerged for all four analyzed samples, WT and the *wrky18 wrky40 wrky33* triple-mutant, before and after elicitation (Figure S3). Merely, the identity of the binding WRKY factors at such sites appear to change upon elicitation as was shown for WRKY18, WRKY40 and WRKY33. These findings are in complete agreement with the observation that upon *B. cinerea* infection WRKY33 also bound only to W-boxes from this set (Liu *et al.*, 2015). Moreover, this finding is also consistent with recent results employing *in vitro* expressed WRKY TFs to interrogate genomic DNA binding using DAP-seq (O'Malley *et al.*, 2016). Although this *in vitro* mapping method detected more W-box-containing regions bound by the various WRKY factors tested, a comparison with our ChIP-seq data revealed very good agreement particularly at major WRKY factor binding sites.

How do the WRKY factors encoded by the constitutively expressed WRKY genes repress gene expression? Although WRKY TFs are capable of acting as activators or repressors (Rushton *et al.*, 2010) a systematic analysis in this respect of the individual WRKY family members has not been performed. Next to such potential intrinsic capabilities, these WRKY TFs may recruit co-repressors that help to fulfill such functions. Interestingly, group I WRKY TFs that are clearly overrepresented among the constitutively expressed WRKY genes have been shown by yeast-2-hybrid studies to preferentially interact with a family of repressors termed VQ proteins (Cheng *et al.*, 2012; Pecher *et al.*, 2014; Jing and Lin, 2015). VQ proteins do not possess DNA-binding capability but interact via their VQ domain with the DNA-binding domain of the WRKY TFs. Transient assays in Arabidopsis protoplasts showed that

several VQ proteins are rapidly phosphorylated and subsequently degraded upon flg22-treatment (Pecher *et al.*, 2014). Thus, it is conceivable that VQ proteins participate as co-repressors of the induced WRKY genes prior to their activation. Interestingly, 17 of the 34 Arabidopsis genes encoding VQ proteins were identified as direct target genes in our ChIP-seq experiments for WRKY18, WRKY40 or WRKY33, and the experiments using the anti-all-WRKY antiserum (Table S7). This suggests that the flg22-induced WRKY factors act in a feed-forward loop to positively regulate the expression of the VQ co-repressor genes whose increased activities subsequently result in the downregulation of the induced WRKY genes. This mode of regulation could ensure a dynamic function by which some early MAMP responses are rapidly activated but subsequently dampened to avoid unnecessary prolonged stress to the plants.

Another major finding of our study was that eliminating three major WRKY factors involved in MTI had little consequence on the overall response of the seedlings to the MAMP flg22 and also did not alter flg22-induced resistance of the plants toward infection with the virulent pathogen *Pst* DC3000. This is very likely due to substitution of these WRKY TFs by other activated WRKY factors at the same functional W-box motifs within the inducible WRKY gene promoters. This result was somewhat unexpected considering the fact that WRKY18, WRKY40 and WRKY33 are predicted to be among the major hubs with a high degree of connectivity within the WRKY network (Choura *et al.*, 2015). It is, however, consistent with the fact that single WRKY mutants rarely display clear altered plant defense phenotypes, and highlights an inherent feature of WRKY TFs, namely their functional redundancy in defense signaling. Recently, both Le Roux *et al.* (2015) and Sarris *et al.* (2015) demonstrated that the *R. solanacearum* effector PopP2 targets multiple WRKY TFs, thereby disrupting their DNA-binding capabilities and transactivating functions required for host defense gene expression. Thus, the redundancy observed within the WRKY TF family probably reflects the need to maintain essential regulatory functions at various levels of the immune network thereby ensuring flexibility and robustness of the system.

EXPERIMENTAL PROCEDURES

Plant materials

For the experiments, plants of the *A. thaliana* ecotype Columbia (Col0) were used. Besides WT plants the triple-mutant *wrky18 wrky33 wrky40*, obtained by crossing of insertion mutants for *WRKY18* (GABI_328G03), *WRKY40* (SLAT collection of dSpm insertion lines; Shen *et al.*, 2007) and *WRKY33* (GABI_324B11), was used. The complementation lines *pWRKY33:WRKY33-HA* (Birkenbihl *et al.*, 2012), *pWRKY18:WRKY18-HA* and *pWRKY40:WRKY40-HA* (Birkenbihl *et al.*, 2017) expressing the transgenes in the respective single-mutants have been described earlier.

To analyze WRKY gene transcript levels of induced WRKY genes the following mutant lines for constitutively expressed WRKY genes were used: *wrky1* (Salk 016911), *wrky2* (GABI_024B05), *wrky3* (SALK_119051), *wrky4* (SALK_073118), *wrky9* (SALK_067122), *wrky14* (SALK_072797), *wrky16* (SALK_001360), *wrky19* (GABI_158D11), *wrky20* (GABI_062C10), Ler *wrky26* (CSHLabs 1704), *wrky32* (GABI_225E04), *wrky57* (SALK_006260), *wrky65* (SALK_050247). The primers used for quantitative polymerase chain reaction (qPCR) are listed in Table S8.

Seedling cultures and flg22-treatment

For seedling cultures, seeds were surface sterilized with ethanol and grown in liquid 1 × MS medium supplemented with 0.5% sucrose and 0.1% of the antibiotic substance claforan. Twelve-day-old seedlings grown in a light chamber under long-day conditions (16 h light/8 h dark) were treated with flg22 or mock-treated by replacing the growth medium with medium containing 1 μM flg22 or not.

Pseudomonas syringae infection of flg22 infiltrated plants

For flg22-induced resistance assays, leaves from 4-week-old plants, grown on Jiffy pots under long-day conditions, were first syringe-infiltrated with 1 μM flg22 or water (mock). After 24 h a *Pst* DC3000 suspension at 1×10^5 cfu ml^{-1} was infiltrated into the pretreated leaves from each genotype. Alternatively, inoculation was carried out by spraying *Pst* at 0.2 OD in 10 mM $MgCl_2$, 0.04% Silvet. Three days after bacterial inoculation, leaf disks (5 mm diameter) were excised from four treated leaves, homogenized and subsequently used to determine *in planta* bacterial titers by plating dilutions of the lysates on fresh NYGA agar plates. Means and standard errors were calculated from six biological replicates.

Chromatin immunoprecipitation-seq experiments

The ChIP-seq experiments and analysis of data employing the complementation lines *pWRKY33:WRKY33-HA*, *pWRKY18:WRKY18-HA* and *pWRKY40:WRKY40-HA* had been conducted earlier and described in Birkenbihl *et al.* (2017), and the data deposited at the GEO repository under the accession number GSE85922.

The ChIP-seq experiments with WT and the *wrky18 wrky33 wrky40* triple-mutant were done in the same manner, but this time using an antiserum raised against the conserved WRKY domain (anti-all-WRKY; Turck *et al.*, 2004) recognizing many different WRKY proteins, again following the modified protocol of Gendrel *et al.* (2005). To prepare the ChIP-seq libraries, the DNA was first amplified by two rounds of linear DNA amplification (LinDA; Shankaranarayanan *et al.*, 2011) and then libraries were constructed with the DNA Smart ChIP-seq kit (Clontech Laboratories, Saint-Germain-en-Laye, France, Cat. No. 634865). The libraries were sequenced at the Max Planck Genome Centre Cologne with an Illumina HiSeq2500, resulting in 10–20 million 150-bp single-end reads per sample.

The ChIP-seq data analysis was also done as described earlier (Birkenbihl *et al.*, 2017), only using a more recent version of Bowtie (version 2.0.5; default settings; Langmead and Salzberg, 2012) for the read alignment. To subsequently remove non-uniquely mapping reads, the alignment output was filtered for mapping quality using SAMtools (version 0.1.18; Li *et al.*, 2009) view with option -q 10. The ChIP-seq data created in this study have been deposited at the GEO repository under the accession number GSE109149.

To obtain more comprehensive peak sets both for the new and the previously published ChIP-seq data, we here included also those peaks in our downstream analyses that were initially

identified by QuEST (Valouev *et al.*, 2008) but rejected by the tool after peak calling.

RNA-seq experiments and quantitative reverse transcription-polymerase chain reaction

The initial WRKY gene transcript level data for WT flg22-treated for 0 h (mock), 1 and 2 h were taken from our previous publication (Birkenbihl *et al.*, 2017), with the data deposited at the GEO repository under the accession number GSE85922.

Additional RNA-seq experiments were performed to investigate differences in WRKY gene transcript levels between WT and the *wrky18 wrky33 wrky40* triple-mutant upon flg22-treatment. For this seedlings of the two genotypes were grown separately for each treatment (mock, 2 h flg22) in three parallel liquid culture sets representing three biological replicates that were also processed and sequenced separately. Total RNA was prepared as described (Birkenbihl *et al.*, 2017) and sequenced at the Max Planck Genome Centre Cologne with an Illumina HiSeq2500, resulting in 20–30 million 100-bp single-end reads per sample. Mapping of the obtained reads to the Arabidopsis genome and data analysis was performed as described earlier (Birkenbihl *et al.*, 2017). The RNA-seq data generated in this study have been deposited at the GEO repository under the accession number GSE109150.

Quantitative reverse transcription-polymerase chain reaction (qRT-PCR) was performed as described earlier using the primers listed in Table S9 (Birkenbihl *et al.*, 2012).

RNA-seq statistical analyses

For the RNA-seq data all statistical analyses were performed using the R package limma (Law *et al.*, 2014) after TMM normalization and log2 transformation of the corresponding read count data. Specifically, a linear model with the explanatory variable 'genotype_time point' (i.e. encoding information on both genotype and time point after treatment) was fitted for each gene using the function lmFit (R package limma). Subsequently, moderated *t*-tests were performed over the different contrasts of interest, comparing the two time points after flg22-treatment with the untreated (0 h) samples for each genotype, and comparing mutant and WT samples at each time point. In all cases, the resulting *P*-values were adjusted for false discoveries due to multiple hypothesis testing via the Benjamini–Hochberg procedure, and expression differences were assumed to be significant if the adjusted *P*-value was smaller than 0.05.

To compare the number of W-boxes in the promoter region between induced and constitutive WRKYs, we performed a non-parametric bootstrap test (with 10 000 iterations).

Immunoprecipitation of WRKY proteins

Twelve-day-old WT seedlings were mock-treated or treated for 2 h with flg22, and 2 g material from each treatment ground in liquid nitrogen. The powder was processed as described in Gendrel *et al.* (2005), in steps 7–17, which resulted in cleared nuclear lysates containing 1% sodium dodecyl sulfate. From each treatment 300 μl lysate was diluted 12-fold with EWB [50 mM Tris pH 7.5, 150 mM NaCl, 10% glycerol, 2 mM EDTA, 5 mM dithiothreitol (DTT)], plus 1% Triton and protease inhibitors, and pre-cleared with 100 μl proteinA agarose for 3 h. Each lysate was subsequently divided into two samples and incubated overnight either with anti-all-WRKY immune serum (Turck *et al.*, 2004) or the corresponding pre-immune serum. The immune complexes were bound to proteinA agarose, washed five times with EWB, eluted twice with 50 μl 0.1% TFA and prepared for MS analysis.

Sample preparation for mass spectrometry

Proteins were denatured in 8 M urea, reduced with 1 mM DTT and alkylated with 5 mM iodoacetamide. Digestion was performed with 300 ng Lysyl endopeptidase (Wako Chemicals, Neuss, Germany) for 1 h at room temperature, followed by an overnight digest with 300 ng trypsin at 37°C. The digests were stopped with 45 μl 10% TFA and loaded on conditioned stage-tips (Rappsilber *et al.*, 2007). The eluates were dried in a vacuum concentrator and dissolved in 2% ACN, 1% TFA prior to LC-MS/MS analysis.

Nano-LC-MS/MS

Peptides were separated using an EASY-nLC1000 UHPLC system (Thermo Fisher Scientific, Waltham, MA, USA) with a 20-cm column, packed in-house with ReproSil-Pur C18-AQ 1.9 μm resin (Dr Maisch GmbH, Tübingen). The column temperature was maintained at 50°C and the column was coupled to a Q Exactive mass spectrometer (Thermo Fisher Scientific) via a nanoelectrospray source. For pull-downs 0.5 μg of total peptides was loaded on the column and separated over a 120-min segmented linear gradient from 0 to 95% buffer B (80% ACN, 0.1% formic acid). The MS was operated in data-dependent mode, survey scans were obtained in a mass range of 300–1750 m/z, at a resolution of 70.000 at 200 m/z and an AGC target value of 3 E6. The 15 most intense ions were selected with an isolation width of 1.3 m/z, fragmented in the HCD cell at 25% collision energy, and the spectra recorded at a target value of 1 E5 and a resolution of 17 500. Peptides with a charge of +1 were excluded from fragmentation, the peptide match and exclude isotope features were enabled, and selected precursors were dynamically excluded from repeated sampling for 30 sec.

Data processing and quantification

Raw data were processed using the MaxQuant software package (version1.5.2.8, http://www.maxquant.org/; Cox and Mann, 2008), and were searched against the Arabidopsis reference proteome (TAIR10_pep_20101214) and an additional database containing contaminants. The search was performed with full trypsin specificity and a maximum of two missed cleavages at a peptide and protein false discovery rate of 1%. Carbamidomethylation of cysteine residues was set as fixed, oxidation of methionine and N-terminal acetylation were set as variable modifications – all other parameters were left at default and LFQ and iBAQ quantification was enabled. The MaxLFQ algorithm integral to MaxQuant was used for LFQ (Cox *et al.*, 2014). The LFQ minimum ratio count was set to 1 and LFQ values were log2 transformed in the Perseus software package (Tyanova *et al.*, 2016). The data are summarized in Data S1.

ACCESSION NUMBERS

The ChIP-seq data generated for WT and *wrky18 wrky40 wrky33* in this study have been deposited at the GEO repository under the accession number GSE109149. The RNA-seq data generated for WT and *wrky18 wrky40 wrky33* in this study have been deposited at the GEO repository under the accession number GSE109150. The MS proteomics data have been deposited to the ProteomeXchange Consortium via the PRIDE partner repository with the dataset identifier PXD008971.

ACKNOWLEDGEMENTS

This work was supported by the Deutsche Forschungsgemeinschaft (DFG) by a grant in the framework of SFB670 Cell Autonomous Immunity (IES and BK), and by the Max Planck Gesellschaft. Technical assistance by Anne Harzen is gratefully acknowledged.

CONFLICT OF INTEREST

The authors declare no conflict of interest.

SUPPORTING INFORMATION

Additional Supporting Information may be found in the online version of this article.

Figure S1. Number of W-boxes in the 1500-bp upstream promoter regions of induced or constitutively expressed WRKY genes.

Figure S2. The *wrky18 wrky40 wrky33* mutant is still proficient in flg22-induced resistance. Spray inoculation with *Pst* DC3000.

Figure S3. IGV images of WRKY gene loci targeted by WRKY factors.

Table S1. Flg22-induced and constitutively expressed WRKY genes

Table S2. Protein levels of the flg22-induced and constitutively expressed WRKY genes acquired by MS

Table S3. WRKY factor binding to WRKY gene loci

Table S4. CHX-induced WRKY genes, based on CHX microarray data (William *et al.*, 2004)

Table S5. Fold change of expression of flg22-inducible WRKY genes in non-treated mutants of constitutively expressed WRKY genes compared with WT seedlings

Table S6. Transcript levels of induced and constitutively expressed WRKY genes in WT and *wrky18 wrky40 wrky33*

Table S7. VQ protein encoding genes targeted by WRKY TFs

Table S8. WRKY gene induction upon flg22-treatment of seedlings compared with induction by *Pst* DC3000 infiltration

Table S9. Primers used for qRT-PCR

Data S1. Proteins identified after immunoprecipitation of nuclear protein extracts using anti-all-WRKY antiserum.

REFERENCES

Andreasson, E., Jenkins, T., Brodersen, P. *et al.* (2005) The MAP kinase substrate MKS1 is a regulator of plant defense responses. *EMBO J.* **24**, 2579–2589.

Banerjee, A. and Roychoudhury, A. (2015) WRKY proteins: signaling and regulation of expression during abiotic stress responses. *Sci. World J.* **2015**, 807 560.

Barah, P., Barah, M.N., Jayavelu, N.D., Sowdhamini, R., Shameer, K. and Bones, A.M. (2016) Transcriptional regulatory networks in *Arabidopsis thaliana* during single and combined stresses. *Nucleic Acids Res.* **44**, 3147–3164.

Berri, S., Abbruscato, P., Faivre-Rampant, O. *et al.* (2009) Characterization of WRKY co-regulatory networks in rice and *Arabidopsis*. *BMC Plant Biol.* **9**, 120.

Birkenbihl, R.P., Diezel, C. and Somssich, I.E. (2012) Arabidopsis WRKY33 is a key transcriptional regulator of hormone and metabolic responses toward *Botrytis cinerea* infection. *Plant Physiol.* **159**, 266–285.

Birkenbihl, R.P., Kracher, B., Roccaro, M. and Somssich, I.E. (2017) Induced genome-wide binding of three WRKY transcription factors during early MAMP-triggered immunity. *Plant Cell* **29**, 20–38.

Brotman, Y., Landau, U., Cuadros-Inostroza, Á., Takayuki, T., Fernie, A.R., Chet, I., Viterbo, A. and Willmitzer, L. (2013) *Trichoderma*-plant root colonization: escaping early plant defense responses and activation of the antioxidant machinery for saline stress tolerance. *PLoS Pathog.* **9**, e1003221.

Brown, R.E., Wilkinson, D.A., Wilkinson, P.M.H., Imran, S.A. and Wilkinson, M. (2012) Superinduction of leptin mRNA in mouse hypothalamic neurons. *Neuroreport* **23**, 900–903.

Cheng, Y., Zhou, Y., Yang, Y. *et al.* (2012) Structural and functional analysis of VQ motif-containing proteins in Arabidopsis as interacting proteins of WRKY transcription factors. *Plant Physiol.* **159**, 810–825.

Cheng, H., Li, H., Deng, Y., Xiao, J., Li, X. and Wang, S. (2015) The WRKY45-2—WRKY13—WRKY42 transcriptional regulatory cascade is required for rice resistance to fungal pathogen. *Plant Physiol.* **167**, 1087–1099.

Choi, C., Hwang, S.-H., Fang, I.R., Kwon, S.I., Park, S.R., Ahn, I., Kim, J.B. and Hwang, D.-J. (2015) Molecular characterization of *Oryza sativa* WRKY6, which binds to W-box-like element 1 of the *Oryza sativa* pathogenesis-related (PR) 10a promoter and confers reduced susceptibility to pathogens. *New Phytol.* **208**, 846–859.

Choura, M., Rebai, A. and Masmoudi, K. (2015) Unraveling the WRKY transcription factors network in *Arabidopsis thaliana* by integrative approach. *Netw. Biol.* **5**, 55–61.

Ciolkowski, I., Wanke, D., Birkenbihl, R. and Somssich, I.E. (2008) Studies on DNA-binding selectivity of WRKY transcription factors lend structural clues into WRKY-domain function. *Plant Mol. Biol.* **68**, 81–92.

Cox, J. and Mann, M. (2008) MaxQuant enables high peptide identification rates, individualized p.p.b.-range mass accuracies and proteome-wide protein quantification. *Nat. Biotechnol.* **26**, 1367–1372.

Cox, J., Hein, M.Y., Luber, C.A., Paron, I., Nagaraj, N. and Mann, M. (2014) Accurate proteome-wide label-free quantification by delayed normalization and maximal peptide ratio extraction, termed MaxLFQ. *Mol. Cell. Proteomics* **13**, 2513–2526.

Cui, H., Tsuda, K. and Parker, J.E. (2015) Effector-triggered immunity: from pathogen perception to robust defense. *Annu. Rev. Plant Biol.* **66**, 487–511.

Dong, J., Chen, C. and Chen, Z. (2003) Expression profiles of the Arabidopsis WRKY gene superfamily during plant defense response. *Plant Mol. Biol.* **51**, 21–37.

Duan, M.-R., Nan, J., Liang, Y.-H., Mao, P., Lu, L., Li, L., Wei, C., Lai, L., Li, Y. and Su, X.-D. (2007) DNA-binding mechanism revealed by high resolution crystal structure of *Arabidopsis thaliana* WRKY1 protein. *Nucleic Acids Res.* **35**, 1145–1154.

Eulgem, T. and Somssich, I.E. (2007) Networks of WRKY transcription factors in defense signaling. *Curr. Opin. Plant Biol.* **10**, 366–371.

Eulgem, T., Rushton, P.J., Schmelzer, E., Hahlbrock, K. and Somssich, I.E. (1999) Early nuclear events in plant defense: rapid gene activation by WRKY transcription factors. *EMBO J.* **18**, 4689–4699.

Eulgem, T., Rushton, P.J., Robatzek, S. and Somssich, I.E. (2000) The WRKY superfamily of plant transcription factors. *Trends Plant Sci.* **5**, 199–206.

Felix, G., Duran, J.D., Volko, S. and Boller, T. (1999) Plants have a sensitive perception system for the most conserved domain of bacterial flagellin. *Plant J.* **18**, 265–276.

Gendrel, A.-V., Lippman, Z., Martienssen, R. and Colot, V. (2005) Profiling histone modification patterns in plants using genomic tiling microarrays. *Nat. Methods* **2**, 213–218.

Guo, D. and Qin, G. (2016) EXB1/WRKY71 transcription factor regulates both shoot branching and responses to abiotic stresses. *Plant Signal. Behav.* **11**, e1150404.

Hsu, F.-C., Chou, M.-Y., Chou, S.-J., Li, Y.-R., Peng, H.-P. and Shih, M.-C. (2013) Submergence confers immunity mediated by the WRKY22 transcription factor in Arabidopsis. *Plant Cell* **25**, 2699–2713.

Hu, Y., Dong, Q. and Yu, D. (2012) Arabidopsis WRKY46 coordinates with WRKY70 and WRKY53 in basal resistance against pathogen *Pseudomonas syringae*. *Plant Sci.* **185–186**, 288–297.

Hussain, A., Li, X., Weng, Y. *et al.* (2018) CaWRKY22 acts as a positive regulator in pepper response to *Ralstonia solanacearum* by constituting networks with CaWRKY6, CaWRKY27, CaWRKY40, and CaWRKY58. *Int. J. Mol. Sci.* **19**, 1426.

Jiang, J. (2015) The 'dark matter' in the plant genomes: non-coding and unannotated DNA sequences associated with open chromatin. *Curr. Opin. Plant Biol.* **24**, 17–23.

Jiang, W. and Yu, D. (2009) Arabidopsis WRKY2 transcription factor mediates seed germination and post-germination arrest of development by abscisic acid. *BMC Plant Biol.* **9**, 96.

Jiang, Y. and Yu, D. (2016) The WRKY57 transcription factor affects the expression of Jasmonate ZIM-domain genes transcriptionally to compromise *Botrytis cinerea* resistance. *Plant Physiol.* **171**, 2771–2782.

Jiang, Y., Liang, G. and Yu, D. (2012) Activated expression of WRKY57 confers drought tolerance in Arabidopsis. *Mol. Plant* **5**, 1375–1388.

Jing, Y. and Lin, R. (2015) The VQ motif-containing protein family of plant-specific transcriptional regulators. *Plant Physiol.* **169**, 371–378.

Kang, X., Li, W., Zhou, Y. and Ni, M. (2013) A WRKY transcription factor recruits the SYG1-like protein SHB1 to activate gene expression and seed cavity enlargement. *PLoS Genet.* **9**, e1003347.

Keilhauer, E.C., Hein, M.Y. and Mann, M. (2015) Accurate protein complex retrieval by affinity enrichment mass spectrometry (AE-MS) rather than affinity purification mass spectrometry (AP-MS). *Mol. Cell. Proteomics* **14**, 120–135.

Kim Do, K., Hwang Cheol, K., Wagley, Y., Law, P.Y., Wei, L.N. and Loh Horace, H. (2011) p38 Mitogen-activated protein kinase and PI3-kinase are involved in upregulation of mu opioid receptor transcription induced by cycloheximide. *J. Neurochem.* **116**, 1077–1087.

Lai, Z., Vinod, K.M., Zheng, Z., Fan, B. and Chen, Z. (2008) Roles of Arabidopsis WRKY3 and WRKY4 transcription factors in plant responses to pathogens. *BMC Plant Biol.* **8**, 68.

Langmead, B. and Salzberg, S.L. (2012) Fast gapped-read alignment with Bowtie 2. *Nat. Methods* **9**, 357–359.

Law, C., Chen, Y., Shi, W. and Smyth, G. (2014) voom: precision weights unlock linear model analysis tools for RNA-seq read counts. *Genome Biol.* **15**, R29.

Le Roux, C., Huet, G., Jauneau, A. *et al.* (2015) A receptor pair with an integrated decoy converts pathogen disabling of transcription factors to immunity. *Cell* **161**, 1074–1088.

Lehti-Shiu, M.D., Panchy, N., Wang, P., Uygun, S. and Shiu, S.-H. (2017) Diversity, expansion, and evolutionary novelty of plant DNA-binding transcription factor families. *Biochim. Biophys. Acta* **1860**, 3–20.

Lewis, L.A., Polanski, K., de Torres-Zabala, M. *et al.* (2015) Transcriptional dynamics driving MAMP-triggered immunity and pathogen effector-mediated immunosuppression in Arabidopsis leaves following infection with *Pseudomonas syringae* pv tomato DC3000. *Plant Cell* **27**, 3038–3064.

Li, R., Yu, C., Li, Y., Lam, T.W., Yiu, S.M. and Kristiansen, K. (2009) SOAP2: an improved ultra-fast tool for short read alignment. *Bioinformatics* **25**, 2078–2079.

Li, S., Fu, Q., Chen, L., Huang, W. and Yu, D. (2011) *Arabidopsis thaliana* WRKY25, WRKY26, and WRKY33 coordinate induction of plant thermotolerance. *Planta* **233**, 1237–1252.

Li, B., Meng, X., Shan, L. and He, P. (2016a) Transcriptional regulation of pattern-triggered immunity in plants. *Cell Host Microbe* **19**, 641–650.

Li, W., Wang, H. and Yu, D. (2016b) Arabidopsis WRKY transcription factors WRKY12 and WRKY13 oppositely regulate flowering under short-day conditions. *Mol. Plant* **9**, 1492–1503.

Liu, S., Kracher, B., Ziegler, J., Birkenbihl, R.P. and Somssich, I.E. (2015) Negative regulation of ABA signaling by WRKY33 is critical for Arabidopsis immunity toward *Botrytis cinerea* 2100. *eLife* **4**, e07295.

Llorca, C.M., Potschin, M. and Zentgraf, U. (2014) bZIPS and WRKYs: two large transcription factor families executing two different functional strategies. *Front. Plant Sci.* **5**, 169.

Lozano-Durán, R., Macho, A.P., Boutrot, F., Segonzac, C., Somssich, I.E. and Zipfel, C. (2013) The transcriptional regulator BZR1 mediates trade-off between plant innate immunity and growth. *eLife* **2**, e00983.

Mao, G., Meng, X., Liu, Y., Zheng, Z., Chen, Z. and Zhang, S. (2011) Phosphorylation of a WRKY transcription factor by two pathogen-responsive MAPKs drives phytoalexin biosynthesis in Arabidopsis. *Plant Cell* **23**, 1639–1653.

Mohanta, T.K., Park, Y.-H. and Bae, H. (2016) Novel genomic and evolutionary insight of WRKY transcription factors in plant lineage. *Sci. Rep.* **6**, 37 309.

Navarro, L., Zipfel, C., Rowland, O., Keller, I., Robatzek, S., Boller, T. and Jones, J.D.G. (2004) The transcriptional innate immune response to flg22. Interplay and overlap with *avr* gene-dependent defense responses and bacterial pathogenesis. *Plant Physiol.* **135**, 1113–1128.

O'Malley, R.C., Huang, S.C., Song, L., Lewsey, M.G., Bartlett, A., Nery, J.R., Galli, M., Gallavotti, A. and Ecker, J.R. (2016) Cistrome and epicistrome features shape the regulatory DNA landscape. *Cell* **165**, 1280–1292.

Pandey, S.P. and Somssich, I.E. (2009) The role of WRKY transcription factors in plant immunity. *Plant Physiol.* **150**, 1648–1655.

Pecher, P., Eschen-Lippold, L., Herklotz, S., Kuhle, K., Naumann, K., Bethke, G., Uhrig, J., Weyhe, M., Scheel, D. and Lee, J. (2014) The *Arabidopsis thaliana* mitogen-activated protein kinases MPK3 and MPK6 target a subclass of 'VQ-motif'-containing proteins to regulate immune responses. *New Phytol.* **203**, 592–606.

Qiao, Z., Li, C.-L. and Zhang, W. (2016) WRKY1 regulates stomatal movement in drought-stressed *Arabidopsis thaliana*. *Plant Mol. Biol.* **91**, 53–65.

Qiu, J.-L., Fiil, B.-K., Petersen, K. *et al.* (2008) Arabidopsis MAP kinase 4 regulates gene expression through transcription factor release in the nucleus. *EMBO J.* **27**, 2214–2221.

Rappsilber, J., Mann, M. and Ishihama, Y. (2007) Protocol for micro-purification, enrichment, pre-fractionation and storage of peptides for proteomics using StageTips. *Nat. Protoc.* **2**, 1896.

Rushton, P.J., Somssich, I.E., Ringler, P. and Shen, Q.J. (2010) WRKY transcription factors. *Trends Plant Sci.* **15**, 247–258.

Sarris, P.F., Duxbury, Z., Huh, S.U. *et al.* (2015) A plant immune receptor detects pathogen effectors that target WRKY transcription factors. *Cell* **161**, 1089–1100.

Schön, M., Töller, A., Diezel, C., Roth, C., Westphal, L., Wiermer, M. and Somssich, I.E. (2013) Analyses of wrky18 wrky40 plants reveal critical roles of SA/EDS1 signaling and indole-glucosinolate biosynthesis for *Golovinomyces orontii* resistance and a loss of resistance toward *Pseudomonas syringae* pv. *tomato* AvrRPS4. *Mol. Plant Microbe Interact.* **26**, 758–767.

Schweizer, F., Bodenhausen, N., Lassueur, S., Masclaux, F.G. and Reymond, P. (2013) Differential contribution of transcription factors to *Arabidopsis thaliana* defence against *Spodoptera littoralis*. *Front. Plant Sci.* **4**, 13.

Shankaranarayanan, P., Mendoza-Parra, M.-A., Walia, M., Wang, L., Li, N., Trindade, L.M. and Gronemeyer, H. (2011) Single-tube linear DNA amplification (LinDA) for robust ChIP-seq. *Nat. Methods* **8**, 565–567.

Shen, Q.-H., Saijo, Y., Mauch, S., Biskup, C., Bieri, S., Keller, B., Seki, H., Ulker, B., Somssich, I.E. and Schulze-Lefert, P. (2007) Nuclear activity of MLA immune receptors links isolate-specific and basal disease-resistance responses. *Science* **315**, 1098–1103.

Sullivan, A.M., Arsovski, A.A., Lempe, J., Bubb, K.L., Weirauch, M.T. and Sabo, P.J. (2014) Mapping and dynamics of regulatory DNA and transcription factor networks in *A. thaliana*. *Cell Rep.* **8**, 2015–2030.

Sun, C., Palmqvist, S., Olsson, H., Borén, M., Ahlandsberg, S. and Jansson, C. (2003) A novel WRKY transcription factor, SUSIBA2, participates in sugar signaling in barley by binding to the sugar-responsive elements of the *iso1* promoter. *Plant Cell* **15**, 2076–2092.

Tao, Z., Liu, H., Qiu, D., Zhou, Y., Li, X., Xu, C. and Wang, S. (2009) A pair of allelic WRKY genes plays opposite roles in rice-bacteria interactions. *Plant Physiol.* **151**, 936–948.

Thorvaldsdóttir, H., Robinson, J.T. and Mesirov, J.P. (2013) Integrative genomics viewer (IGV): high-performance genomics data visualization and exploration. *Brief. Bioinform.* **14**, 178–192.

Tian, X., Li, X., Zhou, W., Ren, Y., Wang, Z., Liu, Z., Tang, J., Tong, H., Fang, J. and Bu, Q. (2017) Transcription factor OsWRKY53 positively regulates brassinosteroid signaling and plant architecture. *Plant Physiol.* **175**, 1337–1349.

Tsuda, K. and Somssich, I.E. (2015) Transcriptional networks in plant immunity. *New Phytol.* **206**, 932–947.

Turck, F., Zhou, A. and Somssich, I.E. (2004) Stimulus-dependent, promoter-specific binding of transcription factor WRKY1 to its native promoter and the defense-related gene *PcPR1-1* in parsley. *Plant Cell* **16**, 2573–2585.

Tyanova, S., Temu, T., Sinitcyn, P., Carlson, A., Hein, M.Y., Geiger, T., Mann, M. and Cox, J. (2016) The Perseus computational platform for comprehensive analysis of (prote)omics data. *Nat. Methods* **13**, 731–740.

Ülker, B. and Somssich, I.E. (2004) WRKY transcription factors: from DNA binding toward biological function. *Curr. Opin. Plant Biol.* **7**, 491–498.

Valouev, A., Johnson, D.S., Sundquist, A., Medina, C., Anton, E., Batzoglou, S., Myers, R.M. and Sidow, A. (2008) Genome-wide analysis of transcription factor binding sites based on ChIP-Seq data. *Nat. Methods* **5**, 829–834.

van Verk, M.C., Pappaioannou, D., Neeleman, L., Bol, J.F. and Linthorst, H.J.M. (2008) A novel WRKY transcription factor is required for induction of PR-1A gene expression by salicylic acid and bacterial elicitors. *Plant Physiol.* **146**, 1983–1995.

William, D.A., Su, Y., Smith, M.R., Lu, M., Baldwin, D.A. and Wagner, D. (2004) Genomic identification of direct target genes of LEAFY. *Proc. Natl Acad. Sci. USA* **101**, 1775–1780.

Xiao, J., Cheng, H., Li, X., Xiao, J., Xu, C. and Wang, S. (2013) Rice WRKY13 regulates crosstalk between abiotic and biotic stress signaling pathways by selective binding to different *cis*-elements. *Plant Physiol.* **163**, 1868–1882.

Xu, X., Chen, C., Fan, B. and Chen, Z. (2006) Physical and functional interactions between pathogen-induced Arabidopsis WRKY18, WRKY40, and WRKY60 transcription factors. *Plant Cell* **18**, 1310–1326.

Yan, L., Liu, Z.-Q., Xu, Y.-H., Lu, K., Wang, X.-F. and Zhang, D.-P. (2013) Auto- and cross-repression of three Arabidopsis WRKY transcription factors WRKY18, WRKY40, and WRKY60 negatively involved in ABA signaling. *J. Plant Growth Regul.* **32**, 399–416.

Yu, Y., Liu, Z., Wang, L. *et al.* (2016) WRKY71 accelerates flowering via the direct activation of *FLOWERING LOCUS T* and *LEAFY* in *Arabidopsis thaliana*. *Plant J.* **85**, 96–106.

Yu, X., Feng, B., He, P. and Shan, L. (2017) From chaos to harmony: responses and signaling upon microbial pattern recognition. *Annu. Rev. Phytopathol.* **55**, 109–137.

Zhang, W., Zhang, T., Wu, Y. and Jiang, J. (2012) Genome-wide identification of regulatory DNA elements and protein-binding footprints using signatures of open chromatin in Arabidopsis. *Plant Cell* **24**, 2719–2731.

Zheng, Z., Qamar, S.A., Chen, Z. and Mengiste, T. (2006) Arabidopsis WRKY33 transcription factor is required for resistance to necrotrophic fungal pathogens. *Plant J.* **48**, 592–605.

Zhou, M., Lu, Y., Bethke, G., Harrison, B.T., Hatsugai, N., Katagiri, F. and Glazebrook, J. (2018) WRKY70 prevents axenic activation of plant immunity by direct repression of SARD1. *New Phytol.* **217**, 700–712.

Zhu, B., Zhang, W., Zhang, T., Liu, B. and Jiang, J. (2015) Genome-wide prediction and validation of intergenic enhancers in Arabidopsis using open chromatin signatures. *Plant Cell* **27**, 2415–2426.

Zipfel, C., Robatzek, S., Navarro, L., Oakeley, E.J., Jones, J.D.G., Felix, G. and Boller, T. (2004) Bacterial disease resistance in Arabidopsis through flagellin perception. *Nature* **428**, 764–767.